Mode-Converted VMS Ore Lens Reflections in Vertical Seismic Profiles and 3D Finite Difference Modeling From Flin Flon, Manitoba, Canada

Dave Melanson[1], Don White[1], Claire Samson[2], Gilles Bellefleur[1], Ernst Schetselaar[1], and Doug Schmitt[3]
[1] *Geological Survey of Canada, 615 Booth Street, Ottawa, Ontario, K1A 0E9*
[2] *Department of Earth Sciences, Carleton University, 1125 Colonel By Drive, Ottawa, Ontario, K1S 5B6*
[3] *Department of Physics, University of Alberta, Edmonton, Alberta, T6G 2E1*

Introduction

Vertical seismic profiles (VSP) were acquired in 2006 as part of a broader seismic exploration program undertaken in the Flin Flon mining camp in Manitoba, Canada (White *et al.*, 2012). The Flin Flon mining camp provides an excellent test-bed to evaluate the ability of VSP methods to detect known volcanogenic massive sulphide (VMS) ore lenses. Three-component VSP data acquired in an open borehole adjacent to the main orebodies of the camp are analyzed here for this purpose. In this case VSP acquisition was limited to the upper half of the borehole. Thus, here we rely on full elastic seismic simulations (Bohlen *et al.*, 2011) conducted for a detailed 3D geological model to correlate the observed VSP reflections with the expected response from the ore lenses. In this project, VSP data was acquired, processed and compared with simulation results of models of increasing complexity to answer the question: Does VSP detect the orebodies?

The Flin Flon Paleoproterozoic greenstone belt is richly endowed with VMS deposits, including the 85.5 Mt Flin Flon-Callinan-777 ore system. Chalcopyrite, pyrrhotite and sphalerite-rich ore lenses are hosted in altered rhyolites of the Millrock member, which lies between the footwall basalts and mafic volcaniclastics of the Flin Flon formation and the hanging wall basalts of the Hidden and Louis formations (Schetselaar *et al.*, 2010). At least three thrust-stacked intervals of the Millrock member contain VMS ore lenses with varying grades, textures and composition of ore. The VMS mining camp in Flin Flon provides a suitable locality to test the proposed approach. Sufficient control on the geometry of the ore lenses and the host crystalline geology exists such that detailed 3D geological models have been previously built. This study focuses on data from open borehole 4Q66W3.

VSP Data Processing

An initial study of the zero-offset dynamite-source data found correlations between strong reflectors along the borehole and some of the primary lithological boundaries obtained from drill cores (Dieteker *et al.*, 2007). The azimuthal orientation of the horizontal sensors during acquisition is variable due to the uncontrolled rotation of the geophone sondes as they are moved from level to level. To achieve consistent alignment of the horizontal component data, two raw horizontal components for each depth level were mathematically rotated to maximize and minimize, respectively, the first arrival P-wave energy from a far-offset dynamite source (DiSiena *et al.*, 1984). This resulted in two horizontal components that are aligned to (H1) and perpendicular to (H2) the direction between the borehole and the far-offset source location (Figure 19). Accounting for the location of the far-offset source location, H1 and H2 are aligned at ~ N68°E and N158°E. Data rotation was

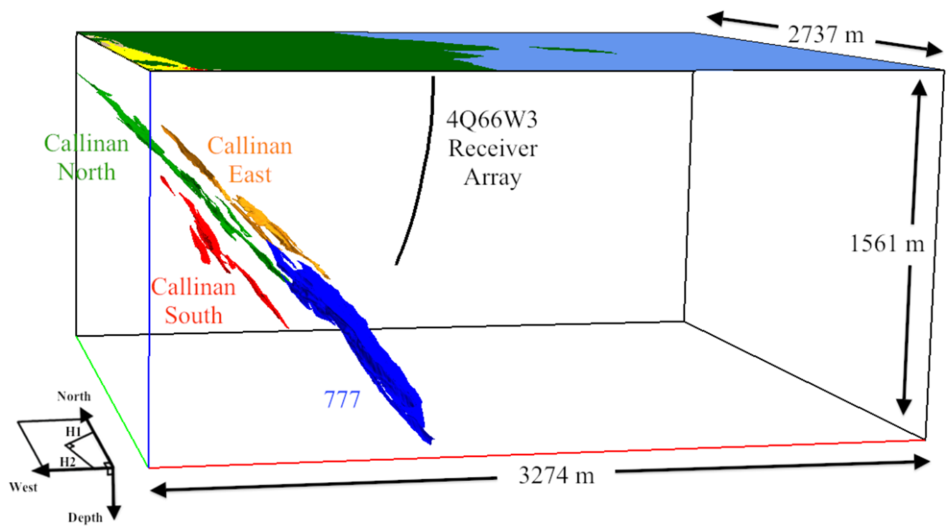

Figure 19. Perspective view of the receiver array and ore zones, based on stratigraphic level located in the 3D voxel model. It should be noted that these zones are not the same as those identified by Hudbay Minerals Inc. (e.g. Tessier and O'Donnell, 2001). Ore zones were used together and in individual simulations to further constrain the origins of ore zone reflections (Melanson, 2014).

Table 7. Physical rock properties used for modeling in this study. 'HPL Core' indicates measurements from core taken at the Dalhousie University High Pressure Laboratory. Other values are based on downhole measurements with the surveyed borehole indicated. All S-wave velocities were calculated using a Vp/Vs ratio from HPL core measurements.

Rock Type	Density (kg/m^3)	From	P-Wave Velocity (m/s)	From	P-wave Impedance (kg/m^2 s)	S-Wave Velocity (m/s)	From	S-wave Impedance (kg/m^2 s)
coherent rhyolite	2740	HPL Core	6008.9	GSC 4Q66	1.65E+07	3609.2	Core Vp/Vs	9.89E+06
mafic fragmentals	2824	GSC 4Q66	6013.7	GSC 4Q66	1.70E+07	3612.1	Core Vp/Vs	1.02E+07
lapilli tuff	2865	HPL Core	6031.9	GSC 4Q66	1.73E+07	3623.1	Core Vp/Vs	1.04E+07
argillite	2830	HPL Core	6180.8	GSC 4Q66	1.75E+07	3712.5	Core Vp/Vs	1.05E+07
massive sulphide ore	4360	HPL Core	6117.9	DGI T7X074	2.67E+07	3674.7	Core Vp/Vs	1.60E+07
meta-basalt	2955	HPL Core	6058.3	GSC 4Q66	1.79E+07	3638.9	Core Vp/Vs	1.08E+07
meta-sandstone	2745	HPL Core	5696.5	DGI 4Q83	1.56E+07	3421.6	Core Vp/Vs	9.39E+06

performed using public domain DSISoft processing software (Beaty *et al.*, 2002).

Each component of the rotated field data was processed individually using GLOBE Claritas software. The application of notch filters was particularly important in reducing the strong electrical noise (60 Hz and harmonics) that can be clearly observed in the raw data. Electrical noise was particularly strong on the vertical component where the 60 Hz and 180 Hz amplitude peaks were ~ 15 – 20 dB above the nominal signal level, whereas amplitude peaks of only 10 – 12 dB and 5 – 7 dB were observed for the H1 and H2 horizontal components, respectively. *F-k* filters were used to remove as much of the direct wavefield as possible. A full-trace amplitude balance and *f-x* deconvolution attenuated random noise and sharpened the reflected wavefield. Finally, a 50 ms static shift was applied to correct a known triggering delay and the data were displayed using automatic gain control (AGC). A similar processing sequence was applied to the horizontal component data, except that the mute window in the *t-x* domain included the direct S-waves as well as the direct P-waves.

Since 4Q66W3 does not intersect any of the ore lenses, corresponding reflections will display an apparent velocity in the shot gathers that is controlled by the 3D geometry of the reflectors and the receiver array. In general, reflections in the field VSP data are discontinuous and can be difficult to trace across the shot gather. The processed shot gathers show very little energy from the direct waves, reduced electrical noise and an enhanced reflected wavefield when compared with the raw shot gathers. The horizontal component shot gathers do not show as much reflectivity as the vertical component, but the observed events are more distinct.

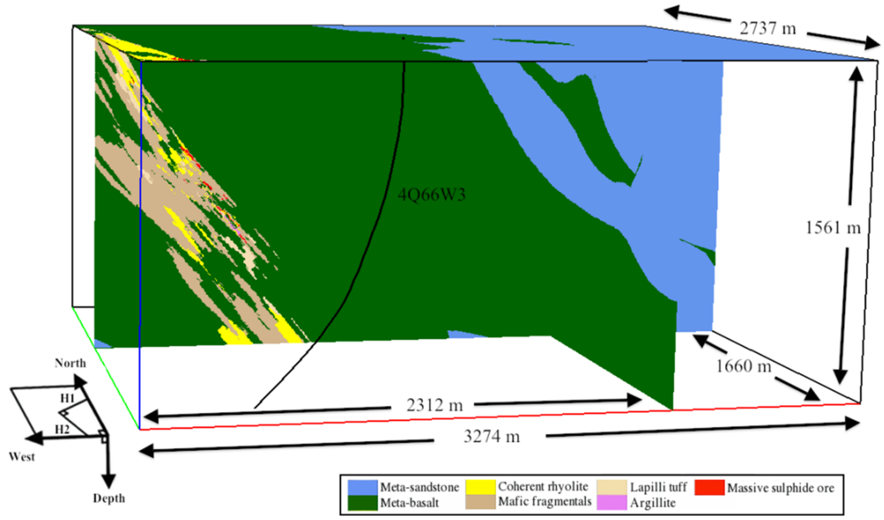

Figure 20: Perspective view of the 3D voxel model displaying all geological units. The ore-hosting Millrock member (yellow and tan) is seen on the left, dipping towards the East, borehole 4Q66W3 is included in black and the edge of the Missi metasedimentary basin (blue) is shown on the right.

3D FINITE DIFFERENCE MODELING

Computer simulations of the seismic response were conducted for detailed 3D geological models to allow comparison with the seismic events observed in the field VSP data, with a particular focus on reflections from the known ore zones (Figure 19). Several raster-based 3D voxel models were constructed based on geological maps, borehole lithological logs and 2D and 3D seismic data (Schetselaar *et al.*, 2010). For each of the 7 rock types included in the various models, density, P-wave velocity

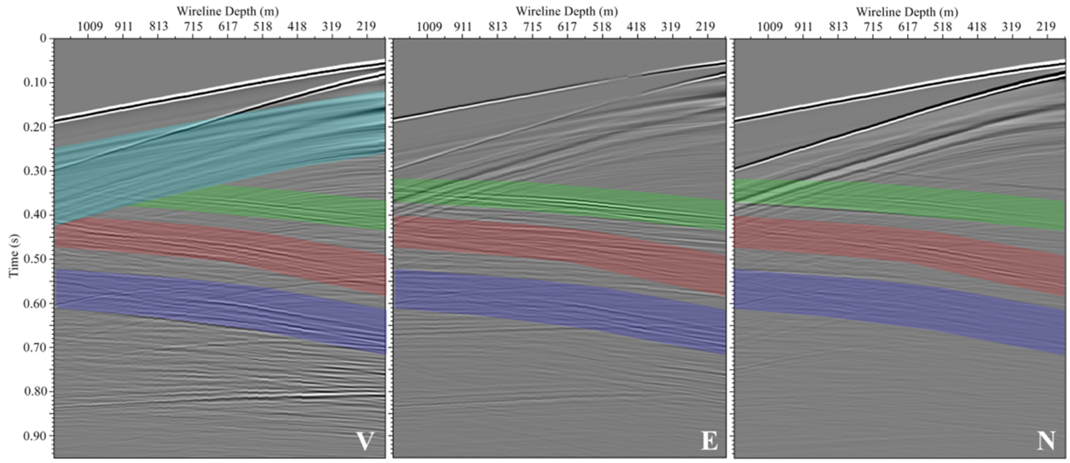

Figure 21: a) vertical (left), b) easting (center) and c) northing (right) particle velocity shot gathers from the lithological model, which includes all 7 major geological units. The light blue region represents downgoing reflections from the Missi basin. There are strong early downgoing reflections (annotated light blue) of surface waves associated with the boundary of the Missi metasedimentary basin, but these do not interfere significantly with the ore zone events. These results indicate that the geometry of and physical properties measured by the field VSP survey will potentially produce an ore zone signature in the data. With these modeling observations in mind, we can now attempt to correlate some reflections between the modeled and field VSP data.

and S-wave velocity values needed to be specified for finite difference modeling (Table 7). These values were determined from laboratory measurements of core samples and downhole geophysical logs from several Flin Flon boreholes including 4Q66W3.

Much of the Callinan deposit has been mined out and backfilled with a low-density material. Intense chlorite-carbonate and clay alteration zones exist and strong variability in mineralogy and texture of the ore zones are known (Tessier and O'Donnel, 2001). We assumed that none of these factors would significantly affect the timing, shape or apparent velocity of observed reflections. Thus, the only differences expected in the field data would be a more complex response and an opposite polarity of reflected waves from the mined out lenses when compared to the modeled VSP data.

The modeling software used in this study was SOFI3D (Bohlen *et al.*, 2011), a 3D viscoelastic finite-difference seismic modeling program. The outputs of each simulation are shot gathers displaying divergence (i.e. P-wave propagation), curl/rotation (i.e. S-wave propagation), pressure and 3-component particle velocities and 3D wavefield visualizations displaying divergence or curl. Comparing shot gathers from simulations with different geological units demonstrated specific seismic events associated with those units as well as their anticipated location in the field VSP data. 3D wavefield visualizations allowed tracing of events back to their point of origin and also identified their mode of propagation (i.e. P-P scattering, P-S conversion, etc.). These observations were then compared to the fully processed field VSP data to identify ore zone events based on their timing, shape and apparent velocities.

Simulations were conducted for a set of models covering a range of geological complexity. The initial simulations were conducted for models where only the ore zones were embedded within a uniform background of meta-basalt (Melanson, 2014). The objective was to understand the fundamental orebody response before considering more detailed models. The complexity of the models was increased for each subsequent simulation culminating in a model which included all 7 of the major lithological units, shown in Figure 20.

In Figure 21, three bands of composite ore zone reflections can be identified corresponding to the PP (green), PS (red) and SS (dark blue) reflected phases based on their timing, apparent velocity and particle motion. These bands are comprised of groups of similar ore zone reflected phases. All of the reflected phases can be identified on each of the geophone components. However, the shear-wave reflections (PS and SS) are most prominent on the vertical-component whereas the PP phase is most prominent on the horizontal components. This is a consequence of the sub-vertical attitude of the wavefront as it approaches the borehole. The PP particle motion, which is orthogonal to the wavefront should be mostly horizontal and a vertical-component of shear would be expected.

DATA COMPARISON AND DISCUSSION

The data from the field VSP survey is considerably more difficult to interpret due to the generally low signal-to-noise ratio and discontinuity of the observed reflections. The vertical component field VSP data (Figure 22a) shows many discontinuous reflections with similar amplitudes, making correlation and identification of specific events difficult. By comparison, the horizontal component field VSP data (Figure 22b, c) show fewer reflections but they appear much

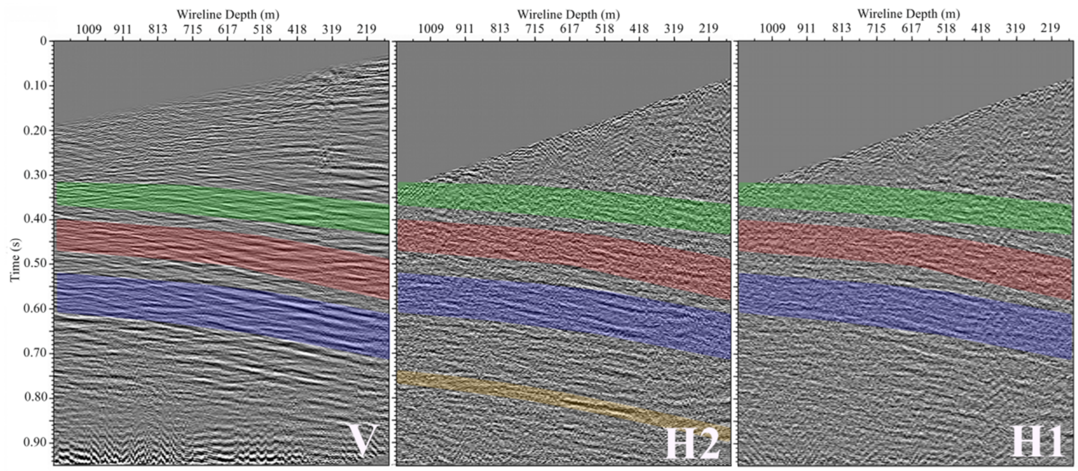

Figure 22. a) vertical (left), b) H2 horizontal (center) and c) H1 horizontal (right) component field data. The orange-annotated event does not correlate with any modeled events.

stronger against background noise levels (particularly on the H2 component, Figure 22b). To allow direct comparison of the field VSP data with the synthetic results, travel time curves for the ore zone events determined from the synthetic shot gathers are overlain on the field data (Figure 22). The following observations can be made: 1) The PP phase (highlighted by the green band in Figure 22) is not apparent on either the vertical- or horizontal- components except perhaps for the shallowest receivers. 2) Calculated travel times and apparent velocities for the PS (red band) and SS (dark blue band) phases show the best correlation with prominent reflections observed on all components of the field data, but particularly for the vertical and H2 components. Based on this comparison, the strongest reflections in the field data correspond to the SS phase from the ore zones. 3) There are a few strong reflections observed between the PS and SS phases on the horizontal field data. These are consistent with the increased complexity in this zone observed on the synthetic data for the lithological model. A single strong event, most noticeable in the H2 horizontal component field data (annotated with orange in Figure 22b) is similar to identified ore zone events, could not be correlated with any modeled event and potentially represents a new exploration target.

Surprisingly, the PP phase from the ore zones is not observed in the field data. In contrast, the SS phase and to a lesser extend the PS phase are observed. The modeling results suggest that all three phases should be observed. The simplest explanation for this is that the magnitude of the P-wave impedance contrast incorporated in the model for the "ore zones" is larger relative to that assigned for the S-wave impedance contrast than is the case for the actual subsurface. This would result in the model predicting a larger PP amplitude relative to the PS and SS phases. As noted earlier, there is significant uncertainty in the physical properties of the ore zones as they have been back-filled with an assumed low-impedance material.

In regard to the phases that are well-observed in the field data (SS and to a lesser extent PS) the modeling results suggest that they should be most prominent on the vertical component. Inspection of the field data in Figure 22 indicates that this is not the case. However, we refrain from ascribing too much significance to this observation as the signal-to-noise ratio is variable amongst the different data components. As noted earlier, the raw vertical-component data had a significantly higher level of electrical noise (by as much as 15 dB) as compared to the raw horizontal component data, and although this noise is greatly attenuated during processing, some residual degradation effect remains.

These observations also demonstrate the importance of 3-component geophones in such applications, as the seismic response has strong directivity and all phases (PP, PS, SS) can have particle motion in any direction due to the complex subsurface geometry and the influence of a deviated borehole. For exploration purposes, the receiver array should be made as long as possible. For example, the 777 deposit was not observed in this study as it was too deep and steeply dipping relative to the receiver array. Also, although detection is possible, it is critical to know where (how far, and in which direction) the target is. With a multi-source VSP, this could potentially be determined based on directivity of arrival and may be the focus of further study.

CONCLUSIONS

The strongest and most identifiable of the ore zone reflections appear to be shear wave reflections (SS) and mode-converted reflections (PS), present on all three components of the field and modeled VSP data. Because of the number and complex shape of the ore zones and the measured reflection coefficients, strong reflected shear waves were expected from their contacts. Such shear waves are best captured by geophones oriented perpendicularly to the wave propagation direction, which explains the strong response observed in the horizontal component field VSP data.

This study shows that VSP surveys have the potential to image VMS lenses in a greenstone host assemblage. The environmental challenge of cultural and electrical noise from an active mine and poor coupling of the geophone tool lead to an overall low signal-to-noise ratio. In this case, the VSP response from the ore lenses is not as prominent as initially anticipated. However, reflections originating from some of the VMS lenses were identified and interpreted in each component of the zero-offset dynamite source VSP data. With the significant investment required for drilling deep targets, it is important to extract as much geological information from boreholes as possible. VSP can provide a means to image dense bodies in the subsurface, even in challenging seismic environments.